


# Preclinical Evaluation of the Accero Stent: Flow Remodelling Effect on Aneurysm, Vessel Reaction and Side Branch Patency

Ruben Mühl-Benninghaus<sup>1</sup>  · Rabie Abboud<sup>1</sup> · Andeas Ding<sup>2</sup> · Stefanie Krajewski<sup>3</sup> · Andreas Simgen<sup>1</sup> · Toshiki Tomori<sup>1</sup> · Hagen Bomberg<sup>4</sup> · Umut Yilmaz<sup>1</sup> · Christoph Brochhausen<sup>5</sup> · Wolfgang Reith<sup>1</sup> · Giorgio Cattaneo<sup>6</sup>

Received: 24 June 2019 / Accepted: 19 September 2019 / Published online: 25 September 2019

© Springer Science+Business Media, LLC, part of Springer Nature and the Cardiovascular and Interventional Radiological Society of Europe (CIRSE) 2019

## Abstract

**Purpose** It has been hypothesized that microstents which are used to prevent coil protrusion in the treatment of cerebral aneurysms may have flow diverting and therefore occlusive effects. In a rabbit elastase aneurysm model, we investigated the aneurysm occlusion rate and vessel reaction of a braided Accero stent prototype with porosity in

the lower range of other available (non-flow-diverter) microstents.

**Methods** Ten aneurysms were induced the right subclavian artery in New Zealand white rabbits and treated with the Accero stent prototype. In each subject, a second stent was implanted in the abdominal aorta to cover the origins of branch arteries. Angiographic follow-up and explantation of the devices and aneurysms for histological analysis were performed after 3 months ( $n = 5$ ) and 6 months ( $n = 5$ ).

**Results** Grades I (< 50%) and II (> 50%) occlusion rates were observed in 9 (90%) and 1 (10%) of ten aneurysms treated with the stent device. The mean reduction in

**Electronic supplementary material** The online version of this article (<https://doi.org/10.1007/s00270-019-02345-z>) contains supplementary material, which is available to authorized users.

✉ Ruben Mühl-Benninghaus  
ruben.mbe@gmail.com

Rabie Abboud  
rabie1991@t-online.de

Andeas Ding  
ading@acandis.com

Stefanie Krajewski  
stefanie.krajewski@uni-tuebingen.de

Andreas Simgen  
andreassimgen@googlemail.com

Toshiki Tomori  
toshiki.tomori@uks.eu

Hagen Bomberg  
hagen.bomberg@uks.eu

Umut Yilmaz  
umut.yilmaz@uks.eu

Christoph Brochhausen  
christoph.brochhausen@klinik.uni-regensburg.de

Wolfgang Reith  
wolfgang.reith@uks.eu

Giorgio Cattaneo  
gcattaneo@acandis.com

<sup>1</sup> Department of Neuroradiology, Saarland University Hospital, Kirrberger Strasse, 66424 Homburg/Saar, Germany

<sup>2</sup> Acandis GmbH, Pforzheim, Germany

<sup>3</sup> Department of Thoracic, Cardiac and Vascular Surgery, University Hospital Tübingen, Tübingen, Germany

<sup>4</sup> Department of Anaesthesiology, Intensive Care Medicine and Pain Medicine, Saarland University Hospital, Homburg/Saar, Germany

<sup>5</sup> Department of Pathology, University of Regensburg, Regensburg, Germany

<sup>6</sup> Institute for Biomedical Engineering, University of Stuttgart, Stuttgart, Germany

contrast filling at 6 months was 42.1% ( $p = .02$ ). Neointima thickness was significantly higher in the subclavian artery than in the abdominal aorta after 3 ( $p = .03$ ), whereas not after 6 months ( $p = .1$ ). No cases of inadequate wall apposition, branch artery occlusion or stent thrombosis were observed.

**Conclusion** The present study showed flow remodelling properties of the device prototype with progredient aneurysm occlusion. A larger in vivo study with induced aneurysm should be done to confirm these results.

**Keywords** Stent · Flow diverter · Aneurysm · Rabbit aneurysm model

## Introduction

Since the introduction of stent-assisted coiling, it was hypothesized that stents, besides preventing coil protrusion, could prevent perfusion of the aneurysm to some extent leading to the concept of endovascular flow diversion. Early studies could validate this concept in in vitro models [1–3]. Very recently this hypothesis was supported by several clinical observations when sole stenting was performed for treatment of intracranial aneurysms with braided stents [4, 5] and even large cell laser-cut stents [6]. Otherwise, because of high porosity of the first-generation laser-cut intracranial stents, in vivo evidence of aneurysm occlusion was not targeted and clinical application as a flow diverting device was limited [7].

Rapid technical progress led to the development of dedicated flow diverters (FDs) with a braided structure and considerably lower porosity than common stents, which have become available for endoluminal vessel reconstruction without the use of coils and were extensively evaluated in in vivo aneurysm models [8, 9]. However, besides the manufacturing differences in the devices, high material density is a potential determinant for thromboembolic complications and side branch occlusion [10–13].

Braiding technology at the same time allowed for manufacturing of stents for coil-assisting procedure with a lower porosity than traditional laser-cut stents, even if considerably higher than in FDs. The purpose of this in vivo study was to evaluate the stand-alone occlusive effect of a fine-meshed braided stent with porosity in the lower range of currently available (non-flow-diverter) microstents in an elastase aneurysm model. Besides the aneurysm occlusion rates, the degree and extent of neointima formation, the patency rate of parent vessel and covered branch arteries were investigated.

## Materials and Methods

The investigated self-expanded stent (SX stent, Acandis, Pforzheim, Germany) is a prototype of the Accero<sup>®</sup> intracranial stent which obtained CE marking for the European Union in 2015 and aimed at coil-assisting technique. The prototype differs from the final Accero stent by different positions of the stent markers and slight different wire loop designs at both distal and proximal ends.

The braided stent consists of a braided structure with a single 50- $\mu$ m-thick nitinol wire including a radiopaque platinum core and radiopaque platinum sleeves distributed in the middle and at both ends of the stent. With ten cells on the circumference, corresponding to 20 wires crossing the stent cross section, and an unconstrained diameter of 4.5 mm, the stent presents a variable porosity and pore density depending on the expansion diameter. If pore density is defined as the reciprocal of the ideal surface of the diamond limited by four wires and comprising the half of the wire width, the pore density amounts to 1.03/0.80/0.84 and 1.13 pores/mm<sup>2</sup> at an unconstrained expanded configuration and in vessels with 4, 3 and 2 mm diameter, respectively. For the same configurations, porosity calculated as ratio between the free surface of the diamond and the surface comprising the half width of the wires corresponds to 84.3%/87.7%/87.1% and 82.7%. At both stent ends, close loops are flared with the aim of an improved vessel apposition. Delivery is performed within a microcatheter of 0.0165" inner diameter. Foreshortening in a vessel with diameter of 2 mm, 3 mm and 4 mm is 7%, 18% and 36%, respectively.

## Animal Experiment

All the experiments were approved by the local animal protection committee (no. 44/13) and conducted in accordance with the animal experiment guidelines. One wide-necked aneurysm with a mean dome-to neck-ratio of  $0.92 \pm 0.23$  was created in each of ten New Zealand white rabbits according the method reported by Altes et al. [14]. Implantation of the SX stent was performed at least 21 days after aneurysm induction [15]. Three days prior to stent placement all animals were treated with aspirin (10 mg/kg orally) and clopidogrel (10 mg/kg orally) daily until the final experiment. The efficacy of dual platelet aggregation inhibition was not tested. Under general anaesthesia, the right femoral artery was surgically exposed and a 4-Fr sheath was inserted. The 2Fr microcatheter Neuroslider 21(Acandis, Pforzheim, Germany) with inner lumen 0.0165" was placed into the aortic arch. Throughout the procedure, 300 U heparin was intravenously administered. For evaluation of the induced aneurysm, digital

subtraction angiography (DSA) was performed. With a standard microguidewire, the Neuroslider 21 microcatheter was manoeuvred beyond the aneurysm neck into the right subclavian artery. Then, the SX stent was unsheathed under road-map guidance. This achieved through slow withdrawal of the delivery microcatheter while, at the same time, holding or gently pushing the delivery wire to achieve complete expansion and wall apposition of the SX stent for 2–3 min. The distal end of the stent was positioned distally to the right vertebral artery, and the proximal part of the stent was deployed within the brachiocephalic trunk. For adequate positioning, the middle radiopaque sleeve of the stent was held on the level of the aneurysm neck during the deployment. After removal of the transport wire, an angiogram of the brachiocephalic trunk was performed. The microcatheter was then retracted and placed in the abdominal aorta for DSA. An additional SX stent was placed in the aorta across the origin of lumbar arteries (Fig. 1C, D). Subsequent DSA was performed to ensure patency of the covered vessels. Endovascular materials were removed, and the femoral artery was ligated.

Subjects were followed for 3 months ( $n = 5$ ) and 6 months ( $n = 5$ ). Under general anaesthesia, the left carotid artery was surgically exposed and a 4-Fr sheath was

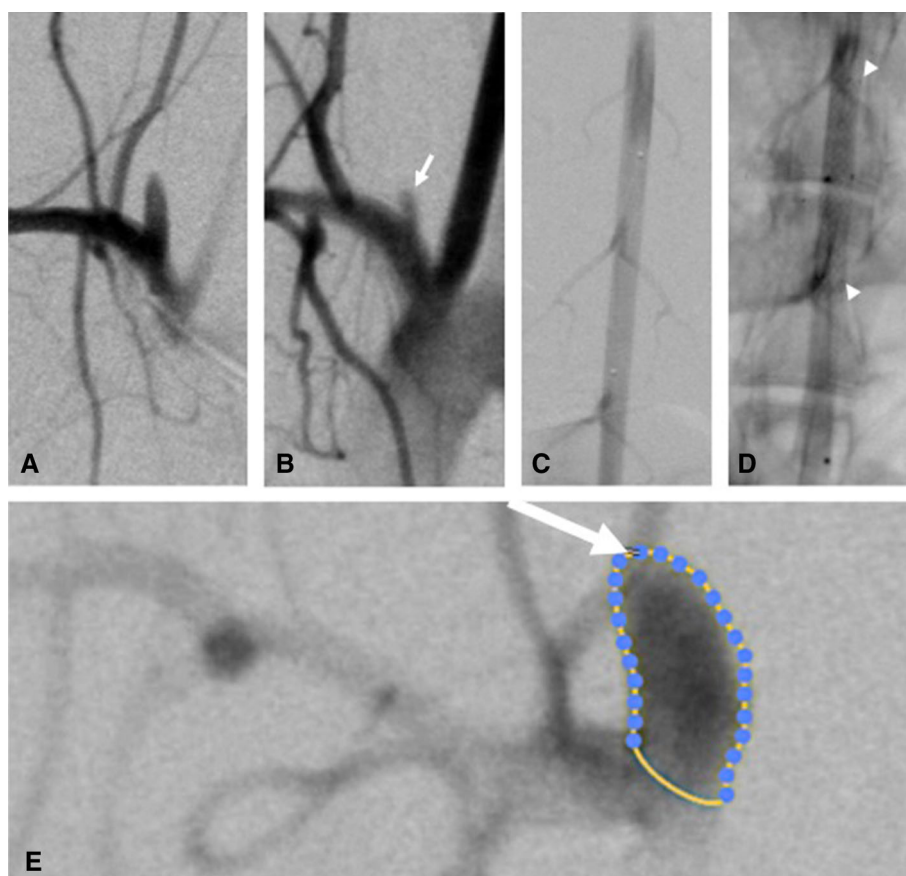
introduced in a retrograde manner with the purpose of better contrast (compared to intravenous injection), and since both femoral arteries were previously sacrificed following the procedure for aneurysm formation and stent implantation, respectively. DSA series were performed as follow-up angiogram, and the animals were sacrificed with a lethal injection of pentobarbital. After harvesting the subclavian artery with the aneurysm and parts of the abdominal aorta, the specimens were fixed in 10% solution of buffered formalin.

## Data Analyses

### Angiographic Evaluation

Three observers analysed angiograms using a five-point grading scheme to evaluate the occlusion of saccular aneurysms in consensus according to Kamran et al. [16] blinded to histology results. Grade 0: no reduction in aneurysmal flow; grade I: less than 50% and grade II: more than 50% flow reduction; grade III: almost complete occlusion; and grade IV: complete occlusion. In addition, the areas of the contrast-filled aneurysms were calculated as follows. The margins of the contrast-filled aneurysms

**Fig. 1** DSA immediately after stent implantation in the subclavian artery (A) and after 3 months follow-up (B) of the same animal shows inadequate occlusion of the aneurysm cavity resulting in grade I occlusion (arrow). DSA of the abdominal artery pre-stent implantation (C) and unsubtracted angiogram 6 months follow-up. Proximal and distal stent markers are highlighted with arrowheads (D). Redrawn margins of the contrast-filled aneurysm sac (E) on posterior–anterior projection on 2D angiogram for calculation of the aneurysm area (exemplarily case, animal no. 9)



were redrawn on posterior–anterior projection on 2D pre-interventional and follow-up angiograms (3 or 6 months) using the pencil tool of OsiriX 6.5.2 (Fig. 1E). Then, the areas of the aneurysms were converted from pixel<sup>2</sup> to mm<sup>2</sup> using a reference object (1 Cent coin), and the reduction in the areas is given as percentage.

Moreover, evaluation of parent vessel thrombosis, stenosis and side branch patency was performed.

### Micro-CT

Micro-CT was performed for assessment of stent integrity and wire fractures. All devices were scanned by high-resolution CT (SkyScan 1172, Belgium). The X-ray tube operated at 75 kV, 10 W and 134  $\mu$ A, with an aluminium filter and a focal spot size of 5  $\mu$ m using a pixel size of 13  $\mu$ m. Volume data were reconstructed with NRecon, volumetric software (1.6.2.0.) and postprocessed with OsiriX 6.5.2.

### Histopathological Processing and Analyses

For each subclavian artery and abdominal aorta, transversal cuts were taken at three different regions (proximal, middle and central) for a total of 60 slices ( $n = 30$  for each follow-up time, respectively). After microscopy (VHX-500F; Keyence; Neu-Isenburg, Germany) and digitization, an experienced pathologist (BD) performed histopathological evaluation, including stent apposition, neointima thickness, inflammation and potential foreign body reaction surrounding the stent struts and the presence of thrombotic material.

Morphometric measurements were performed as follows. Thickness of the neointima = distance between the outer surface of each strut and the luminal border. Neolumen = distance from luminal border to the opposite luminal border. Former vessel lumen = distance from the outside of a strut to the opposite outside of the strut across the vessel diameter. Diameter stenosis =  $(\text{Neolumen} \div \text{Former lumen}) \times 100$ . For each parameter, maximum and minimum values were measured and average was calculated.

### Statistical Analyses

Statistical analysis was performed using SPSS 20.0. Continuous variables are expressed as means and standard deviations (SD). Differences between the groups were compared with Student's *t*-test (or Welch's *t*-test when variance was inhomogeneous). The statistical significance of changes from baseline within each group was tested with paired *t*-test. Statistical significance was accepted at two-sided  $p \leq .05$ .

## Results

### Angiography

Aneurysm characteristics and dimensions of harbouring arteries are given in Table 1.

In all cases, the delivery and deployment of the devices were successful. No case of stent migration or inadequate wall apposition was observed.

The mean diameter of the stented aorta was 3.8 mm  $\pm$  0.49 mm in the 3 months' group and 3.5 mm  $\pm$  0.33 mm in the 6 months group.

The mean area of the aneurysms in the 3 months group was 17.31  $\pm$  7.48 mm<sup>2</sup> before treatment and 13.45  $\pm$  6.33 mm<sup>2</sup> after treatment (reduction 22.5%, non-significant,  $p = .06$ ). The mean area of the aneurysms in the 6 months group was 25.4  $\pm$  23.87 mm<sup>2</sup> before treatment and 15.37  $\pm$  12.85 mm<sup>2</sup> after treatment (reduction 42.1%, significant  $p = .02$ ) (Fig. 2A, B). Overall occlusion rates of grades I and II were noted in 9 (90%) and 1 (10%) of ten aneurysms, respectively. In the 3 months group, grade I occlusion rate was noted in all five cases (Fig. 1A, B). In the 6 months group, grade I occlusion rate was noted in four cases (80%) and grade II occlusion in one case (20%).

All branch arteries (e.g. vertebral, renal or lumbar arteries) covered by the SX stent remained patent at follow-up. Mean diameter of vertebral, renal and lumbar artery origin was 1.3  $\pm$  0.1, 2.3  $\pm$  0.3 mm and 1.2  $\pm$  0.2 mm, respectively. Angiographically, no stenosis in parent vessels or stent thrombosis was assessed.

### Micro-CT

All stents were intact in both subclavian and aorta. No wire fractures or distortion was assessed. A light bulging of the stents in the central part was observed in all aorta specimens, while in the subclavian artery, a tapering with continuous diameter reduction extended from the proximal to the distal part, according to the vessel geometry. A representative picture of both specimens in the same animal is shown in Fig. 3A, B.

### Histology

Histologically, in all analysed tissue sections stent material was observed at the interface between the media and the neointima leading to complete wall apposition in all cases (Fig. 3C, D).

The neointima thickness of the stent harbouring vessels was significantly higher in the subclavian artery than in the abdominal aorta at follow-up 3 months (119.3  $\pm$  59.0  $\mu$ m

**Table 1** Aneurysm and harbouring artery characteristics

Time, months	No.	Parent vessel size, p/d (mm)	Neck size (mm)	Transverse diameter (mm)	Height (mm)	D/N ratio
3	1	2.6/2.1	3.32	2.77	6.34	0.8
	2	2.8/2.2	3.35	2.49	6.16	0.7
	3	2.8/2.3	4.71	3.07	10.81	0.7
	4	2.5/2.6	3.04	1.98	5.93	0.7
	5	3.1/2.3	2.34	2.77	4.80	1.2
6	6	3.1/2.3	4.68	3.42	8.65	0.7
	7	2.9/2.3	3.12	2.87	5.96	0.9
	8	2.9/2.1	2.01	2.73	6.74	1.4
	9	3.2/2.4	4.25	4.50	8.18	1.1
	10	3.5/2.5	4.96	3.79	10.09	0.8

*p/d* proximal/distal, *D/N* dome/neck

vs  $53.0 \pm 7.0 \mu\text{m}$ , Fig. 2C). This difference was not significant after 6 months ( $92.0 \pm 40.2 \mu\text{m}$  vs  $49.2 \pm 10.3$ , Fig. 2E). Stenosis grade was significantly higher in the subclavian artery compared with abdominal aorta at follow-up 3 months ( $p = .03$ ); after 6 months there was no significant difference between aorta and subclavian artery ( $p = .6$ ) (Fig. 2D, F).

In the regions of the aneurysm neck, incomplete neointima formation with scattered neointima islands was observed over the stent wires. Inflammation and foreign body reaction were seen in 1 of 30 slices, both at 6 months follow-up (3.3%). Calcification islands were observed in 4 and 11 slices at 3 and 6 months (13.3% and 36.7%), (Fig. 4).

## Discussion

In this study, we report the in vivo evaluation of a fine-meshed braided stent as a sole device in the treatment of wide-neck aneurysms without coiling. In comparison with common FDs like Pipeline embolization device (PED, Medtronic, Irvine, California, USA), Silk flow diverter (SFD, Balt Extrusion, Montmorency, France) or Derivo (Acandis, Pforzheim, Germany), the investigated SX stent is characterized by a higher porosity.

Since use of FDs can be associated with thromboembolic events and might cause delayed brain parenchymal lesions [17, 18], recent clinical studies underline the potential role of high-porosity implant, i.e. for small diameter vessels and vessels with high perforator density. In the study of Matsuda et al. [19], low-neck metal coverage correlated to less perforator coverage in a comparison between a stent and a flow diverter in a cadaver. Möhlenbruch et al. [20] presented the results of the implantation of a 0.021" compatible FD with porosity of

70% in a multicentre clinical study, showing an aneurysm occlusion rate amounting to 100% at 12 months despite a 12% rate of thrombus related events.

Besides FD treatment, the use of multiple stents in telescoping technique is another option for aneurysm treatment. Xu et al. [21] showed the feasibility of this procedure in a retrospective clinical study. Aneurysm occlusion rate was achieved in 80% in the case series. But this technique holds the risk of thromboembolic events and in-stent stenosis due to the increased material and overlying struts.

The main idea of our investigation was to assess the flow remodelling performance and vessel reaction of the Accero stent prototype with less material coverage and deliverability within a 0.0165" microcatheter in an experimental in vivo model. Due to the decrease in the metal-to-artery ratio compared to FDs, the SX stent could potentially reduce thromboembolic complications.

Some in vitro and numerical investigations were previously performed to assess intra-aneurysmal fluid dynamical effect of implants with different porosities, including intracranial stents and flow diverters [22, 23]. Although a certain flow modification was proven also for high-porosity stents, biological factors triggering intra-aneurysmal clot formation and vessel reconstruction are obviously neglected in these models.

In both follow-up 3 and 6 months, we observed an incomplete aneurysm occlusion with a reduction in aneurysm filling in both groups, being significant after 6 months follow-up compared to baseline. The progressive occlusion can be explained by the increase in induced scattered neointima islands covering the device struts across the aneurysm neck (Fig. 4). These results support the findings of several clinical studies using low-profile braided stents as a stent monotherapy in aneurysm treatment. In Cagnazzo et al. [5], a 70% complete aneurysm

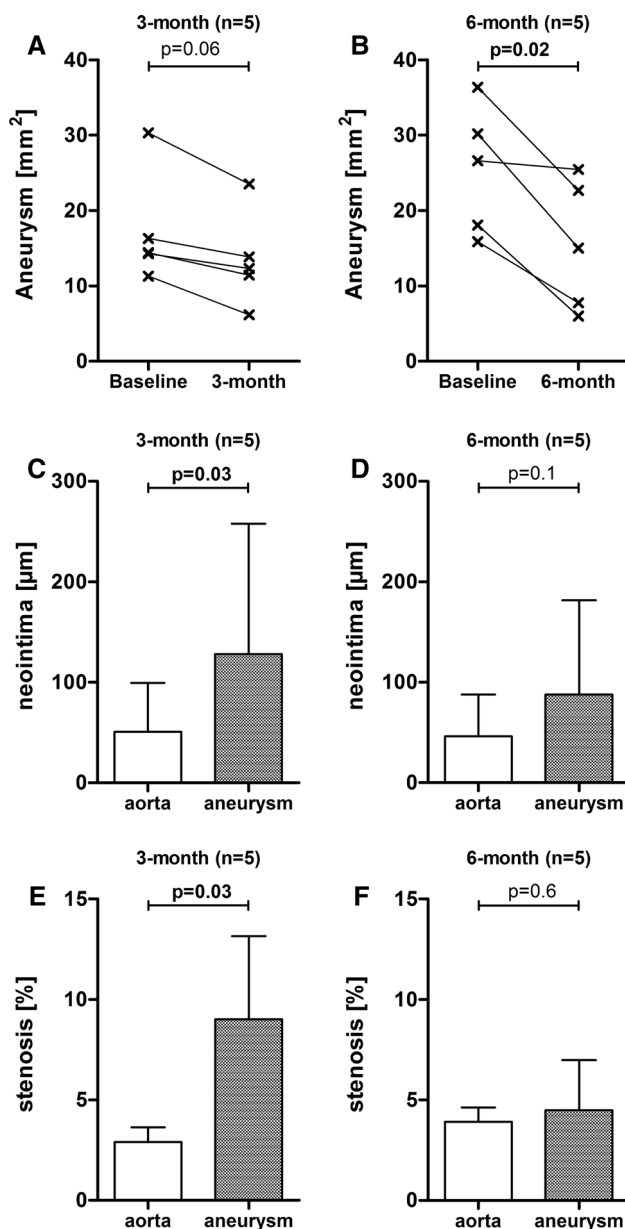


**Fig. 2** A and B Area of the aneurysms measured on posterior-anterior projection of DSA, baseline (initial aneurysm area before stent implantation) and after 3 months (A) and 6 months (B) follow-up. Results of neointima thickness of the stented aorta and subclavian artery (defined as aneurysm) after 3 months (C) and 6 months (E). D and F show their corresponding stenosis after each time point

treated with a braided stent was reported. In Kim et al. [24], implantation of laser-cut stents led to a complete occlusion of 37.5% of aneurysms treated.

Previous investigations with state-of-the-art FDs in similar rabbit models with comparable aneurysm dimensions achieved high aneurysm occlusion rates. Kallmes et al. [25] observed complete occlusion in 40% and 80% of aneurysms at 3 and 6 months follow-up using implants with 70% porosity. Sadasivan et al. [26] compared three

devices with porosity between 65 and 70%, achieving higher occlusion rate for implants with higher pore density. In Ley et al [27], two devices with porosity 65% and 80% showed a significantly higher rate of complete occlusion at a lower porosity.

Also Wang et al. [28] showed a positive correlation between aneurysm occlusion rate and metal coverage measured by micro-CT.

The investigated device presents porosity in the lower range of currently available intracranial stents. According to the calculation presented before, a mean subclavian artery diameter of 2 mm to 3 mm leads to porosity between around 82.8% and 87.1% in our study. For comparison, Cho et al. [29] investigated the porosity of different intracranial stents at 0.5 mm oversizing, amounting to 86–88.5% for braided, 90% for an open-cell laser cut and 95% for a close-cell laser-cut stent.

The higher porosity compared to FDs is presumably responsible for a weaker or rather slower intra-aneurysmal flow reduction and thus occlusion rate. A previous in vitro study showed a relationship between flow diverter porosity and intra-aneurysmal thrombus formation, hypothesizing (1) a material-triggered thrombus initiation and (2) a thrombus growing dependent on intra-aneurysmal stagnation points [30]. However, in our study the area of residual aneurysm filling was progressively decreasing and significantly lower at 6 months follow-up compared to baseline, indicating the potential for a slow aneurysm occlusion. Longer follow-up results would be needed to evaluate the further progression of the occlusion.

The histological evaluation revealed a slight foreign body reaction without significant inflammation. The focal calcification observed in some slides was also reported in previous studies [31, 32].

The higher neointima thickness and diameter stenosis in the subclavian artery compared to the stented aorta is in agreement with previous studies [8, 33] and is presumably caused by the increased metal coverage and different mechanical behaviour due to the device oversizing in small vessel diameter. Furthermore, the devices in the subclavian arteries are exposed to a higher shear stress due to the movement of the legs of the animals.

In Kallmes et al., implantation of flow diverter in the subclavian artery resulted in a neointima and stenosis grade ranging between 100 and 200 ± 100 μm and between 17 and 23% at 6 months follow-up. In Sadasivan et al., neointima thickness was between 129 and 175 μm depending on the implanted flow diverter. In Ley et al., neointima thickness was between 125 and 138 μm in different subclavian regions, with the stenosis grade amounting to 7.3% to 8.3% at 6 months follow-up. Considering the similarity of the animal models, the lower neointima thickness and stenosis rate in the investigated

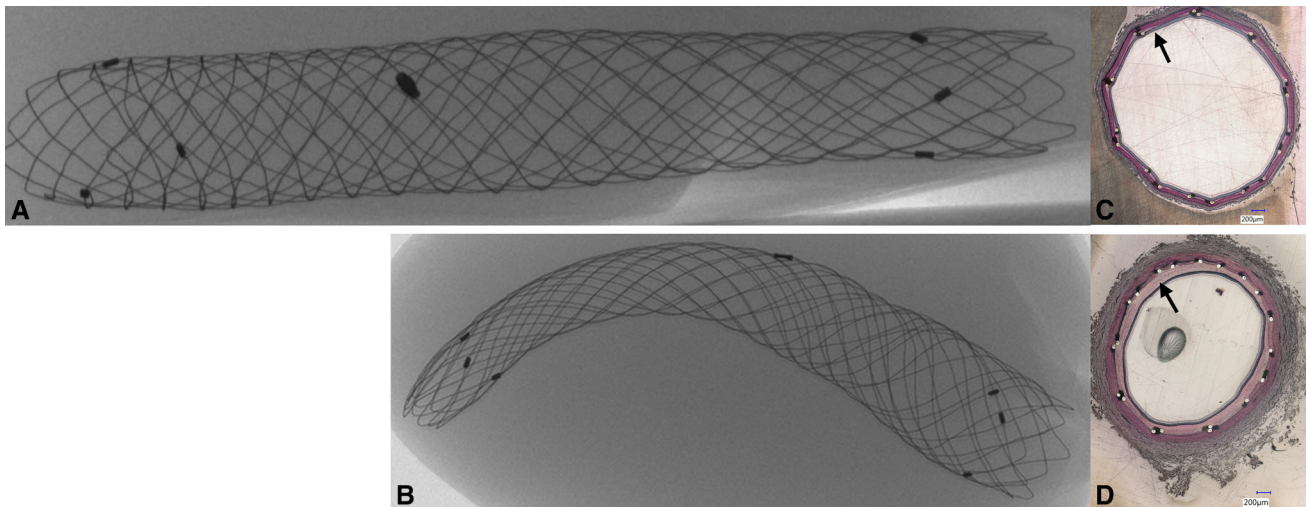


**Fig. 3** CT scans of the Accero stent prototype explanted from the abdominal aorta (A) and subclavian artery (B) from the same animal after 3 months. Photomicrograph (H&E) of neointima (arrows) being thinner in the abdominal aorta (C) than in the subclavian artery (D)

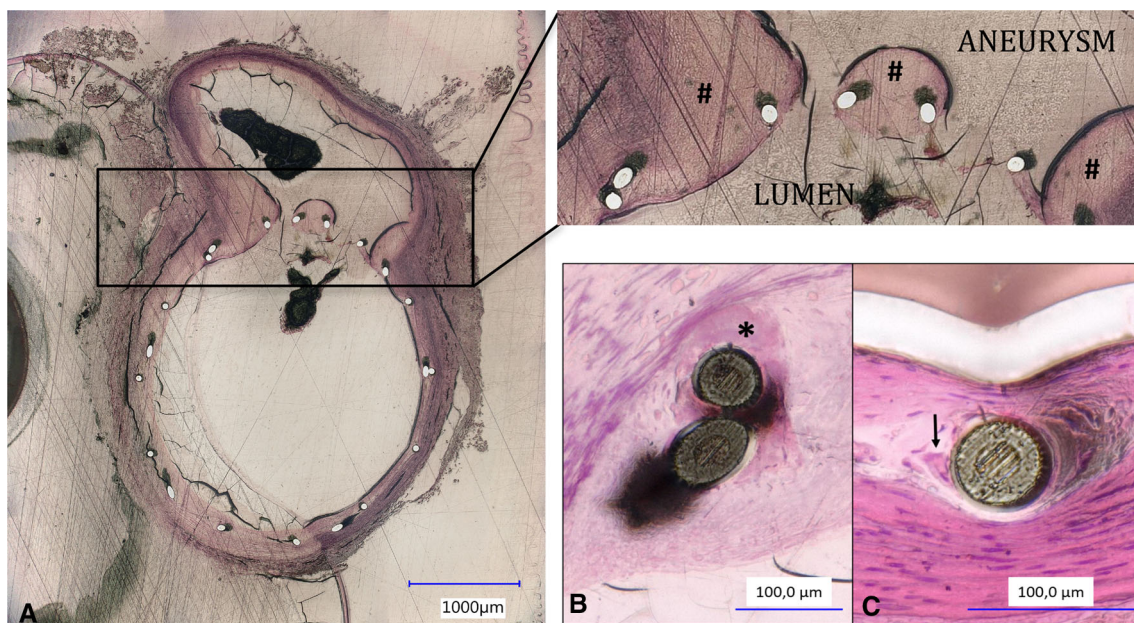


**Fig. 4** Photomicrograph (H&E) of subclavian artery. Neointima islands (hash) at the aneurysm neck at 3 months follow-up (A). Beginning calcification (starlet) (B) and foreign body giant cell (arrow) (C) after 6 months follow-up

stent can be presumably ascribed to the lower metal density and thus lower vessel stress.

Our preclinical study had some limitations. We did not include a control group of untreated aneurysms or a group of aneurysms treated with commercial available FDs, since experience with this animal model at our department has proven patency of untreated aneurysms and adequate occlusion rates after 6 months with flow diverting implants [27, 32]. The study population was small. The induced aneurysms in a rabbit model differ from spontaneously grown intracranial aneurysms in humans regarding morphological properties such as size and neck diameter as

pointed out by Kallmes [25]. Further, the induced aneurysms are more similar to a side-wall aneurysm. Flow diversion properties of the tested stent may differ in the treatment of bifurcation aneurysms due to hemodynamic variations.

## Conclusion

The Accero stent is biocompatible. The implantation of the Accero stent alone, without coil occlusion, does not allow a reliable occlusion of the target aneurysms. Using the same

model (elastase aneurysms in rabbits), a comparison of coiling alone versus Accero-assisted coiling would allow a better understanding of the potential benefit of said stent, beyond the mechanical coil retention.

**Funding** This work was supported by the German Ministry of Economic Affairs and Energy (Grant No KF2335804AJ2) and partially funded by Acandis GmbH, Pforzheim, Germany.

#### Compliance with Ethical Standards

**Conflict of interest** Giorgio Cattaneo was engineer at the company Acandis GmbH until August 2019, Andreas Ding is engineer at the company Acandis GmbH (Pforzheim, Germany). Both served as proctors during this study.

**Ethical Approval** All applicable international, national and/or institutional guidelines for the care and use of animals were followed. All procedures performed in studies involving animals were in accordance with the ethical standards of the institution or practice at which the studies were conducted. This study obtained approval by the local animal protection committee (No. 44/13).

#### References

- Lieber BB, Stancampiano AP, Wakhloo AK. Alteration of hemodynamics in aneurysm models by stenting: influence of stent porosity. *Ann Biomed Eng.* 1997;25(3):460–9.
- Han PP, Albuquerque FC, Ponce FA, MacKay CI, Zabramski JM, Spetzler RF, et al. Percutaneous intracranial stent placement for aneurysms. *J Neurosurg.* 2003;99(1):23–30. <https://doi.org/10.3171/jns.2003.99.1.0023>.
- Wang C, Tian Z, Liu J, Jing L, Paliwal N, Wang S, et al. Flow diverter effect of LVIS stent on cerebral aneurysm hemodynamics: a comparison with enterprise stents and the pipeline device. *J Transl Med.* 2016;14(1):199. <https://doi.org/10.1186/s12967-016-0959-9>.
- Aydin K, Barbuoglu M, Sencer S, Berdikhojajev M, Coskun B, Akpek S. Flow diversion with low-profile braided stents for the treatment of very small or uncoilable intracranial aneurysms at or distal to the circle of Willis. *AJNR Am J Neuroradiol.* 2017;38(11):2131–7. <https://doi.org/10.3174/ajnr.A5362>.
- Cagnazzo F, Cappucci M, Dargazanli C, Lefevre PH, Gascou G, Riquelme C, et al. Flow-diversion effect of LEO stents: aneurysm occlusion and flow remodeling of covered side branches and perforators. *AJNR Am J Neuroradiol.* 2018;39(11):2057–63. <https://doi.org/10.3174/ajnr.A5803>.
- Pumar JM, Lete I, Pardo MI, Vazquez-Herrero F, Blanco M. LEO stent monotherapy for the endovascular reconstruction of fusiform aneurysms of the middle cerebral artery. *AJNR Am J Neuroradiol.* 2008;29(9):1775–6. <https://doi.org/10.3174/ajnr.A1155>.
- Lanzino G, Wakhloo AK, Fessler RD, Hartney ML, Guterman LR, Hopkins LN. Efficacy and current limitations of intravascular stents for intracranial internal carotid, vertebral, and basilar artery aneurysms. *J Neurosurg.* 1999;91(4):538–46. <https://doi.org/10.3171/jns.1999.91.4.0538>.
- Kallmes DF, Ding YH, Dai D, Kadirvel R, Lewis DA, Cloft HJ. A new endoluminal, flow-disrupting device for treatment of saccular aneurysms. *Stroke J Cereb Circ.* 2007;38(8):2346–52. <https://doi.org/10.1161/STROKEAHA.106.479576>.
- Ahlhelm F, Roth C, Kaufmann R, Schulte-Altendorneburg G, Romeike BF, Reith W. Treatment of wide-necked intracranial aneurysms with a novel self-expanding two-zonal endovascular stent device. *Neuroradiology.* 2007;49(12):1023–8. <https://doi.org/10.1007/s00234-007-0281-6>.
- Kulcsar Z, Houdart E, Bonafe A, Parker G, Millar J, Goddard AJ, et al. Intra-aneurysmal thrombosis as a possible cause of delayed aneurysm rupture after flow-diversion treatment. *AJNR Am J Neuroradiol.* 2011;32(1):20–5. <https://doi.org/10.3174/ajnr.A2370>.
- Yavuz K, Geyik S, Saatci I, Cekirge HS. Endovascular treatment of middle cerebral artery aneurysms with flow modification with the use of the pipeline embolization device. *AJNR Am J Neuroradiol.* 2014;35(3):529–35. <https://doi.org/10.3174/ajnr.A3692>.
- Brinjikji W, Lanzino G, Cloft HJ, Siddiqui AH, Boccardi E, Cekirge S, et al. risk factors for ischemic complications following pipeline embolization device treatment of intracranial aneurysms: results from the IntrePED study. *AJNR Am J Neuroradiol.* 2016;37(9):1673–8. <https://doi.org/10.3174/ajnr.A4807>.
- Pumar JM, Banguero A, Cuellar H, Guimaraens L, Masso J, Miralbes S, et al. treatment of intracranial aneurysms with the SILK embolization device in a multicenter study. *Retrospect Data Anal Neurosurg.* 2017. <https://doi.org/10.1093/neuros/nyw123>.
- Altes TA, Cloft HJ, Short JG, DeGast A, Do HM, Helm GA, et al. 1999 ARRS Executive Council Award. Creation of saccular aneurysms in the rabbit: a model suitable for testing endovascular devices. American Roentgen Ray Society. *AJR Am J Roentgenol.* 2000;174(2):349–54. <https://doi.org/10.2214/ajr.174.2.1740349>.
- Fujiwara NH, Cloft HJ, Marx WF, Short JG, Jensen ME, Kallmes DF. Serial angiography in an elastase-induced aneurysm model in rabbits: evidence for progressive aneurysm enlargement after creation. *AJNR Am J Neuroradiol.* 2001;22(4):698–703.
- Kamran M, Yarnold J, Grunwald IQ, Byrne JV. Assessment of angiographic outcomes after flow diversion treatment of intracranial aneurysms: a new grading schema. *Neuroradiology.* 2011;53(7):501–8. <https://doi.org/10.1007/s00234-010-0767-5>.
- Safain MG, Roguski M, Heller RS, Malek AM. Flow diverter therapy with the pipeline embolization device is associated with an elevated rate of delayed fluid-attenuated inversion recovery lesions. *Stroke J Cereb Circ.* 2016;47(3):789–97. <https://doi.org/10.1161/STROKEAHA.115.010522>.
- Zhou G, Su M, Yin YL, Li MH. Complications associated with the use of flow-diverting devices for cerebral aneurysms: a systematic review and meta-analysis. *Neurosurg Focus.* 2017;42(6):E17. <https://doi.org/10.3171/2017.3.FOCUS16450>.
- Matsuda Y, Chung J, Keigher K, Lopes D. A comparison between the new low-profile visualized intraluminal support (LVIS Blue) stent and the flow redirection endoluminal device (FRED) in bench-top and cadaver studies. *J Neurointerv Surg.* 2017. <https://doi.org/10.1136/neurintsurg-2017-013074>.
- Mohlenbruch MA, Kizilkilic O, Killer-Oberpfalzer M, Baltacioglu F, Islak C, Bendszus M, et al. multicenter experience with FRED Jr flow re-direction endoluminal device for intracranial aneurysms in small arteries. *AJNR Am J Neuroradiol.* 2017;38(10):1959–65. <https://doi.org/10.3174/ajnr.A5332>.
- Xu D, Zhang C, Wang T, Wang C, Kallmes DF, Lanzino G, et al. Evaluation of enterprise stent-assisted coiling and telescoping stent technique as treatment of supraclinoid blister aneurysms of the internal carotid artery. *World Neurosurg.* 2018;110:e890–6. <https://doi.org/10.1016/j.wneu.2017.11.119>.
- Bouillot P, Brina O, Ouared R, Lovblad KO, Farhat M, Pereira VM. Particle imaging velocimetry evaluation of intracranial stents in sidewall aneurysm: hemodynamic transition related to the stent design. *PLoS one.* 2014;9(12):e113762. <https://doi.org/10.1371/journal.pone.0113762>.



23. Suzuki T, Takao H, Fujimura S, Dahmani C, Ishibashi T, Mamori H, et al. Selection of helical braided flow diverter stents based on hemodynamic performance and mechanical properties. *J Neurointerv Surg*. 2017;9(10):999–1005. <https://doi.org/10.1136/neurintsurg-2016-012561>.
24. Kim YJ, Ko JH. Sole stenting with large cell stents for very small ruptured intracranial aneurysms. *Interv Neuroradiol J Peripher Neuroradiol Surg Proced Relat Neurosci*. 2014;20(1):45–53. <https://doi.org/10.15274/INR-2014-10007>.
25. Kallmes DF, Ding YH, Dai D, Kadirvel R, Lewis DA, Cloft HJ. A second-generation, endoluminal, flow-disrupting device for treatment of saccular aneurysms. *AJNR Am J Neuroradiol*. 2009;30(6):1153–8. <https://doi.org/10.3174/ajnr.A1530>.
26. Sadasivan C, Cesar L, Seong J, Rakian A, Hao Q, Tio FO, et al. An original flow diversion device for the treatment of intracranial aneurysms: evaluation in the rabbit elastase-induced model. *Stroke J Cereb Circ*. 2009;40(3):952–8. <https://doi.org/10.1161/STROKEAHA.108.533760>.
27. Ley D, Mühl-Benninghaus R, Yilmaz U, Korner H, Cattaneo GF, Mailander W, et al. The Derivo embolization device, a second-generation flow diverter for the treatment of intracranial aneurysms, evaluated in an elastase-induced aneurysm model. *Clin Neuroradiol*. 2015. <https://doi.org/10.1007/s00062-015-0493-9>.
28. Wang K, Huang Q, Hong B, Li Z, Fang X, Liu J. Correlation of aneurysm occlusion with actual metal coverage at neck after implantation of flow-diverting stent in rabbit models. *Neuroradiology*. 2012;54(6):607–13. <https://doi.org/10.1007/s00234-011-0922-7>.
29. Cho SH, Jo WI, Jo YE, Yang KH, Park JC, Lee DH. Bench-top comparison of physical properties of 4 commercially-available self-expanding intracranial stents. *Neurointervention*. 2017;12(1):31–9. <https://doi.org/10.5469/neuroint.2017.12.1.31>.
30. Gester K, Luchtefeld I, Busen M, Sonntag SJ, Linde T, Steinseifer U, et al. In vitro evaluation of intra-aneurysmal, flow-diverter-induced thrombus formation: a feasibility study. *AJNR Am J Neuroradiol*. 2016;37(3):490–6. <https://doi.org/10.3174/ajnr.A4555>.
31. Dai D, Ding YH, Kadirvel R, Rad AE, Lewis DA, Kallmes DF. Patency of branches after coverage with multiple telescoping flow-diverter devices: an in vivo study in rabbits. *AJNR Am J Neuroradiol*. 2012;33(1):171–4. <https://doi.org/10.3174/ajnr.A2879>.
32. Simgen A, Ley D, Roth C, Yilmaz U, Korner H, Mühl-Benninghaus R, et al. Evaluation of a newly designed flow diverter for the treatment of intracranial aneurysms in an elastase-induced aneurysm model, in New Zealand white rabbits. *Neuroradiology*. 2013. <https://doi.org/10.1007/s00234-013-1296-9>.
33. Simgen A, Ley D, Roth C, Cattaneo GF, Mühl-Benninghaus R, Müller A, et al. Evaluation of occurring complications after flow diverter treatment of elastase-induced aneurysm in rabbits using micro-CT and MRI at 9.4 T. *Neuroradiology*. 2016;58(10):987–96. <https://doi.org/10.1007/s00234-016-1730-x>.

**Publisher's Note** Springer Nature remains neutral with regard to jurisdictional claims in published maps and institutional affiliations.